Electrical conductance of carbon nanotori in contact with single-wall carbon nanotubes

Y. Y. Chou and G.-Y. Guo
Department of Physics, National Taiwan University, Taipei 106, Taiwan

Lei Liu, C. S. Jayanthi, and S. Y. Wu
Department of Physics, University of Louisville, Louisville, Kentucky 40292

(Received 12 April 2004; accepted 4 May 2004)

The realization of the potential of carbon nanotori as elements of nanoscale devices based on their recently predicted unusual properties requires a thorough understanding of contacting these nanostructures. We carried out a series of calculations of the electric conductance of carbon nanotori contacted by single-wall carbon nanotubes to shed light on the effects of the geometry as well as the chemistry of the contacts. The relaxed structures of the contacted nanotori were determined by an order-N nonorthogonal tight-binding molecular dynamics scheme. The conductance was calculated using the Landauer-Büttiker formula based on a π-orbital Hamiltonian. We found that the conductance of the contacted carbon nanotorus is very sensitive to the transparency (chemistry) of the contacts. We also found that the equivalence (chemistry as well as geometry) of the contacts plays an important role in the transport properties. For example, a difference in the right contact and left contact will diminish the constructive quantum interference of the transmission as compared to the situation when the two contacts are equivalent. This conclusion is general and is expected to be applicable for any metallic contacts to the contacted carbon nanotori. © *2004 American Institute of Physics*. [DOI: 10.1063/1.1766415]

I. INTRODUCTION

Recent reports on the observation and the synthesis of closed carbon nanotube (NT) rings[1,2] have generated renewed interest in the study of the magnetic properties of carbon nanotube-based nanostructures.[3,4] For example, it was predicted theoretically that nanotori formed from metal-l NTs (Ref. 5) [e.g., the metallic zigzag single-wall carbon nanotubes (SWCNT)] may exhibit giant paramagnetic moments at any radius while those formed from metal-2 NTs (Ref. 5) (e.g., the armchair SWCNT) may exhibit this characteristics only at (selected) magic radii.[4] These discoveries suggest the potential for using carbon nanotori (CNTRI) in devices such as ultrasensitive magnetic sensors. However, to facilitate a wider use of this unusual nanostructure, it is imperative to have a clear understanding of the effect of connecting a carbon nanotorus (CNTR) as a component in a device to other components of the system. In this paper, we report our study of contacting a CNTR with contacts of different degrees of transparency to shed light on the effects of the geometry and the chemistry of the contact on the transport properties of CNTR. We found the conductance of the contacted CNTR to be dependent on both the degree of transparency and the equivalence of the contacts.

II. THE SYSTEMS

In Ref. 4, it was shown that a metallic CNTR could be formed from any metal-1 SWCNT. On the other hand, a metal-2 SWCNT could form a metallic CNTR only if its circumference, $L=pT$, where p is an integer and T the translation vector of the SWCNT, is such that p is a multiple of 3. Otherwise, the resulting CNTR is a small-gap semiconductor. To develop a complete picture of the transport properties of the contacted CNTR, we chose, as our working examples, to study two CNTRI, one formed from the metal-1 SWCNT (12,0) and the other from the metal-2 (6,6) SWCNT of similar diameter. An earlier investigation by us on the stability of nanotori using a quantum mechanics based molecular dynamics (MD) scheme implemented with a nonorthogonal tight-binding (NOTB) Hamiltonian had indicated that a (5,5) nanotorus will undergo a change from an elastic deformation to the development of kinks at a critical diameter of ~4 nm (or ~50 unit cells).[6] Therefore, we selected four cases, namely, a (12,0)/3600 CNTR [a CNTR formed from a (12,0) zigzag SWCNT containing 3600 carbon atoms or 75 unit cells], a (12,0)/3648 CNTR containing 76 unit cells, a (6,6)/3648 CNTR [a CNTR formed from a (6,6) armchair SWCNT containing 3648 carbon atoms or 152 unit cells], and a (6,6)/3672 CNTR containing 153 unit cells, for our study because they are expected to be stable and without any kinks. To understand how the degree of transparency of the contacts affects the transport properties of a contacted CNTR, we used the semi-infinite zigzag (6,0) SWCNT to contact the CNTR. On the one hand, the (6,0) SWCNT was chosen as the contacts for the following reasons: (1) the same type of chemical bonding will prevail between atoms in the contact [the (6,0) SWCNT] and those in the sample [the (12,0) SWCNT-based or the (6,6) SWCNT-based CNTR], thus allowing for the possibility of transparent contacts; (2) because the Fermi energy for the (6,0) SWCNT is the same as that of the (12,0) SWCNT while it is different from that of the (6,6) SWCNT, the contact between the (6,0) SWCNT and the (12,0) SWCNT-based CNTRI can be construed as an almost transparent contact, while that between the (6,0)

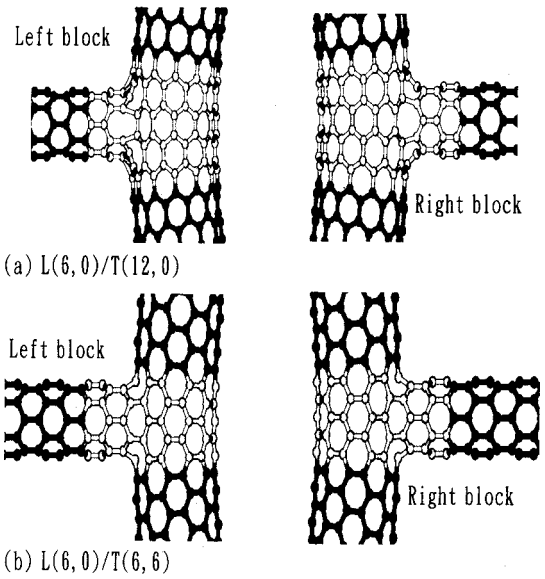

FIG. 1. The schematic representations of the junction regions: (a) L(6,0)-T(12,0)/3600 and (b) L(6,0)-T(6,6)/3648. The atoms and bonds in light shade in the right and left regions represent the right junction and left junction, respectively, whose LDOS are plotted in Figs. 2 and 3.

SWCNT and the (6,6) SWCNT-based CNTR a less transparent contact; and (3) a consistent determination of the relaxed configuration for the CNTR contacted by a SWCNT can be carried out in a more convenient manner. On the other hand, the information extracted from the study of SWCNT-contacted CNTRI can be used to understand the transport properties of metal-contacted CNTRI for those metals that can form metal carbide with the carbon atom.

III. STRUCTURAL RELAXATION AND THE CALCULATION OF LOCAL DENSITY OF STATES

We setup the initial configuration of the (6,0) SWCNT-contacted CNTR by forming two T junctions at the opposite ends of the CNTR. In the case of (6,6) CNTRI, the T junctions can be formed by the introduction of, at each junction, four seven-edged polygons, two each at both sides of the exterior joint. For (12,0) CNTRI, the introduction of four seven-edged polygons at each junction will, in addition, create two seven-edged polygons, one at the top and the other at the bottom of the connection, that anchor the connection between the (12,0) CNTR and the (6,0) SWCNT lead. The initial configuration created in this manner was then relaxed, using an order-N NOTB-MD (O(N)-NOTB-MD) scheme[7] because of the size of the system under consideration. Two schematic representations of the relaxed right and left junctions of (6,0) SWCNT-contacted CNTRI, one for the (12,0)/3600 CNTR and the other for the (6,6)/3648 CNTR, are shown in Fig. 1.

We have formed the junctions for the four CNTRI mentioned earlier by contacting them with the semi-infinite (6,0)-SWCNT leads and relaxed the initial configurations of the contacted CNTR (CNTR plus the connections between the leads and the CNTR) to obtain the corresponding relaxed structures for those contacted-CNTRI. Once the structure of the (6,0) SWCNT-contacted CNTR (CCNTR) was determined, we constructed the Hamiltonian of the relaxed structure (the sample), H_S, using the simple π-orbital Hamiltonian to facilitate the calculation of the transport properties of the SWCNT-contacted CNTR since the π-orbital Hamiltonian has been shown to give a reliable representation of the electronic structure of SWCNTs.[4,5] To gain an insight of the electronic structure of the relaxed CCNTR, it is important to analyze the local density of states (LDOS) of relevant sections of the relaxed structure. The LDOS of a certain section I of the relaxed structure, $\rho_I(E)$, can be determined by[8]

$$\rho_{\mathrm{I}}(E) = -\frac{1}{N_{\mathrm{I}}\pi}\lim_{\varepsilon\to 0}\sum_{i\in I} R_{ii}(E+i\varepsilon), \tag{1}$$

where the Green's function $R(E)$ is defined by

$$R(E) = \{E - H_{\mathrm{S}} - V_{\mathrm{SL}}\Delta_{\mathrm{L}}V_{\mathrm{LS}} - V_{\mathrm{SR}}\Delta_{\mathrm{R}}V_{\mathrm{RS}}\}^{-1}, \tag{2}$$

with

$$\Delta_{\mathrm{L(R)}} = (E - H_{\mathrm{L(R)}})^{-1}, \tag{3}$$

the summation over the atomic site index i running through all the atoms in the particular section I of the relaxed structure, N_{I} being the total number of atoms in the section under consideration, E the energy, $V_{\mathrm{SL(SR)}}$ the coupling between the sample and the left (right) lead, and $H_{\mathrm{L(R)}}$ the Hamiltonian of the left (right) lead. In Figs. 2 and 3, we present the LDOS for the region of the right junction (RJ), the region of the left junction (LJ), the region in the middle portion of the torus (MT), and the CCNTR (the torus plus the two junctions) for the four relaxed CCNTRI, respectively. In Fig. 2(a), the LDOSs for the RJ and LJ of the (6,0) SWCNT, contacted CNTR (6,6)/3648 [L(ead)(6,0)-T(orus)(6,6)/3648 CCNTR] are shown, respectively. Also shown in Fig. 2(c) is the DOS of the SWCNT (6,0). Since the (6,6)/3648 CNTR is composed of 152 unit cells, the configuration for the RJ is equivalent to that of the LJ. Therefore, their respective LDOSs are identical as can be seen from Fig. 2(a). Because of the finiteness of the L(6,0)-T(6,6)/3648 CCNTR, the DOSs exhibit oscillations about their respective average. It can be seen that the most prominent features in the LDOS of RJ (LJ) are the second set of Van Hove peaks (at $E\approx -2.7$ and $E\approx 2.7$ eV) in the DOS of the (6,0) SWCNT (the lead). Traces of the first three sets of van Hove peaks (at $E\approx -1.4$ and 1.4 eV; -2.3 and 2.3 eV; -2.7 and 2.7 eV) in the DOS of the (6,6) SWCNT [see Fig. 2(c)] can also be found in the LDOS of the RJ (LJ). Another discernable feature in the LDOS of the RJ (LJ) is in the vicinity of $E\approx 0.8$ eV. We have identified this feature as associated with the seven-edged polygon defects at the connection between the (6,6)/3648 CNTR and the (6,0) SWCNT. In Fig. 2(a), the LDOS of a block in the middle portion of the (6,6)/3638 CNTR, MT, is also shown. It can be seen that the main features of the DOS of the (6,6) SWCNT [Fig. 2(c)] are reproduced in the LDOS of the MT. One interesting footnote is that the (6,6)/3648 CNTR is composed of 152 unit cells. Since the (6,6) SWCNT is a metal-2 SWCNT and 152 is not a multiple of 3, the corresponding (6,6)/3648 CNTR is therefore a small-gap semiconductor. A check of the LDOS of MT indeed shows a small gap at the Fermi energy ($E=0$). Figure

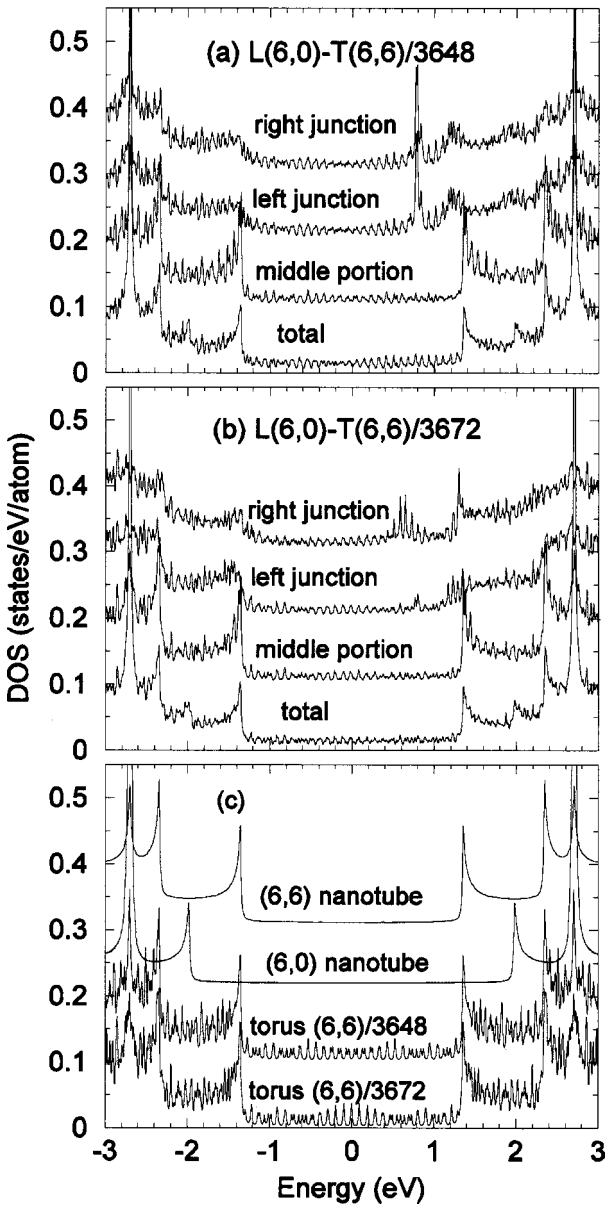

FIG. 2. LDOS of the right junction, the left junction, the middle portion, and the (6,0) SWCNT-contacted CNTR for the L(6,0)-T(6,6) carbon nanotorus junctions with (a) 3648 atoms and (b) 3672 atoms in the torus, respectively. LDOS of the middle portion, the left junction, and the right junction have been displaced upwards by 0.1, 0.2, and 0.3 states/eV-atom, respectively: (c) DOS of SWCNTs (6,6) and (6,0) as well as CNTRI (6,6)/3648 and (6,6)/3672. DOSs of CNTR (6,6)/3648, SWCNTs (6,0) and (6,6) have been displaced upwards by 0.1, 0.2, and 0.3 states/eV-atom, respectively.

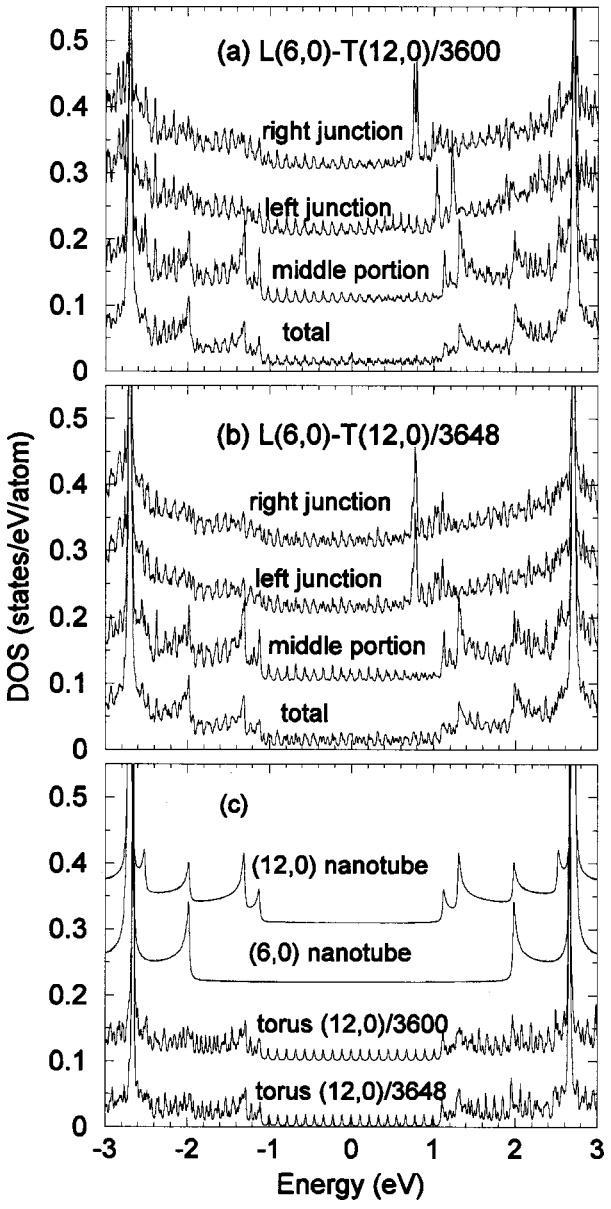

FIG. 3. LDOS of the right junction, the left junction, the middle portion, and the (6,0) SWCNT-contacted CNTR for the L(6,0)-T(12,0) carbon nanotorus junctions with (a) 3600 atoms and (b) 3648 atoms in the torus, respectively. LDOS of the middle portion, the left junction, and the right junction have been displaced upwards by 0.1, 0.2, and 0.3 states/eV-atom, respectively. (c) DOS of SWCNTs (12,0) and (6,0) as well as CNTRI (12,0)/3600 and (12,0)/3648, respectively. DOS of CNTR (12,0)/3600, SWCNTs (6,0) and (12,0) have been displaced upwards by 0.1, 0.2, and 0.3 states/eV-atom, respectively.

2(a) also shows the LDOS of the L(6,0)-T(6,6)/3648 CCNTR. It contains all the essential features of the SWCNT (6,0) and the (6,6)/3648 CNTR, including the small gap at the Fermi energy.

In Fig. 2(b), the same set of LDOSs as those given in Fig. 2(a) but for the L(6,0)-T(6,6)/3672 CCNTR are shown. It should be noted that the (6,6)/3672 CNTR is composed of 153 unit cells. Since 153 is a multiple of 3, therefore the (6,6)/3672 CNTR is a metallic CNTR. Furthermore, because it contains an odd number of unit cells, the configuration of its RJ is different from that of its LJ at the opposite end. These characteristics of the (6,6)/3672 CNTR are clearly seen in Fig. 2(b). For example, an examination of Figs. 2(b) reveals that the LDOS of the RJ and that of the LJ are different. Although they both still exhibit features similar to those associated with the (6,0)-SWCNT contact and the (6,6)/3672 CNTR (such as the prominent second set of Van Hove peaks of the (6,0) SWCNT and the first three sets of Van Hove peaks of the (6,6) SWCNT) just as seen in Fig. 2(c), the feature associated with the configuration of the seven-edged polygon defects appears differently in the LDOSs of the LJ and RJ of the L(6,0)-T(6,6)/3672 CCNTR. While the defect feature still appears in the neighborhood of $E \approx 0.8$ eV in the LDOS of LJ of the L(6,0)-T(6,6)/3672 CCNTR, it is much less prominent compared to the corre-

sponding feature of the L(6,0)-T(6,6)/3648 CCNTR. In the LDOS of the RJ of the L(6,0)-T(6,6)/3672 CCNTR, this feature appears more diffused and shifted to the neighborhood of 0.6 eV, as compared to the feature at 0.8 eV in the LJ or RJ of the L(6,0)-T(6,6)/3648 CCNTR. The LDOS of the MT of the L(6,0)-T(6,6)/3672 CCNTR shown in Fig. 2(b) reflects basically the essential features of the (6,6)/3672 CNTR. In particular, the DOS at the Fermi energy ($E=0$) does not vanish, an indication that the (6,6)/3672 CNTR is a metallic CNTR. Figure 2(b) also shows the LDOS of the L(6,0)-T(6,6)/3672 CCNTR. It can be seen that this LDOS possesses the prominent features of the (6,6)/3672 CNTR as well as those of the (6,0) SWCNT. Specifically the DOS at the Fermi energy is not zero, indicating that the contacts have not changed the metallic behavior of the (6,6)/3672 CNTR.

Both of the two (12,0) SWCNT-based CNTRI are metallic CNTRI. In the case of the (12,0)/3600 CNTR, it is composed of 75 unit cells. Therefore, the configuration of the RJ of the (6,0)-(12,0)/3600 CCNTR is different from that of the LJ. On the other hand, the (12,0)/3648 CNTR is composed of 76 unit cells. Hence the configuration of the RJ of the L(6,0)-T(12,0)/3648 CCNTR is the same as that of its LJ. The similar as well as contrasting characteristics of these two CCNTRI are expected to reveal themselves in their corresponding LDOSs. Indeed these characteristics can be seen in the features in the LDOSs shown in Figs. 3(a) and 3(b). For example, the LDOS of the RJ of the L(6,0)-T(12,0)/3600 CCNTR composed of 75 unit cells shown in Fig. 3(a), while similar to the two identical LDOSs of the RJ and LJ [Fig. 3(b)] of the L(6,0)-T(12,0)/3648 CCNTR with 76 unit cells, is different from that of its LJ [Fig. 3(a)]. The difference shows up in the feature associated with the seven-edged defect configuration. This feature occurs at $E \approx 0.8$ eV in the LDOS of the RJ [Fig. 3(a)] of the L(6,0)-T(12,0)/3600 CCNTR and seems to have merged with the feature associated with the (12,0) SWNT at $E \approx 1.0$ eV in the LDOS of its LJ [Fig. 3(a)]. Both the MT of the L(6,0)-T(12,0)/3600 CCNTR [Fig. 3(a)] and that of the L(6,0)-T(12,0)/3648 CCNTR [Fig. 3(b)] exhibit all the essential features of the DOS of the (12,0) SWCNT and they are similar to each other. The DOS at Fermi energy is not zero for both MTs, reflecting the fact that both CNTRI [(12,0)/3600 and (12,0)/3648] are metallic. Figures 3(a) and 3(b) also show the LDOSs of the L(6,0)-T(12,0)/3600 CCNTR and L(6,0)-T(12,0)/3648 CCNTR, respectively. As expected, they both exhibit the features associated with the (6,0) SWCNT and the (12,0) SWCNT and they are very similar. The DOS at the Fermi energy is nonzero in both cases, indicating that the contacts do not affect the metallic nature of the two CNTRI.

IV. ELECTRICAL CONDUCTANCE

With the electronic structure of the set of four CCNTRI determined and analyzed, we proceeded to calculate the conductance of these CCNTRI. The conductance was calculated using the Landauer-Büttiker formula[9]

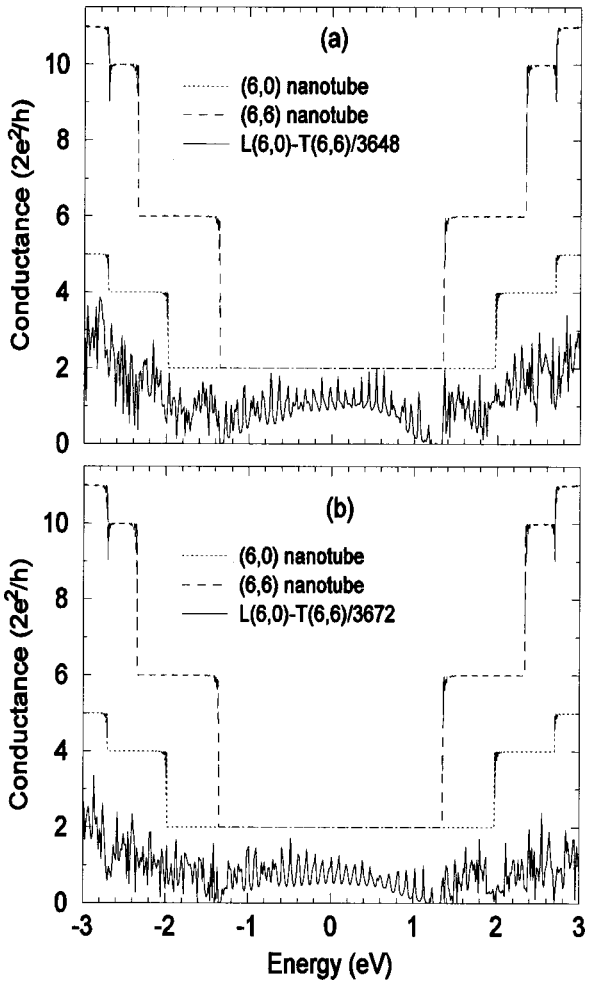

FIG. 4. Conductance of the L(6,0)-T(6,6) contacted CNTRI with (a) 3648 atoms and (b) 3672 atoms in the torus, respectively. Also shown are the conductance of the SWCNTs (6,0) and (6,6).

$$G = \frac{2e^2}{h}\mathrm{Tr}(\Gamma_L R_S^r \Gamma_R R_S^a), \tag{4}$$

where the advanced (retarded) Green's function of the sample (the CCNTR), $R_S^{a(r)}$, is simply $R_S^a = R_S(E+i\varepsilon)$ [$R_S^r = R_S(E-i\varepsilon)$] of Eq. (2), and $\Gamma_{L(R)} = i\{V_{SL(R)}\Delta_{L(R)}^r V_{L(R)S} - V_{SL(R)}\Delta_{L(R)}^a V_{L(R)S}\}$. In Figs. 4(a) and 4(b), the conductance of the (6,0)-(6,6)/3648 CCNTR and that of the (6,0)-(6,6)/3672 CCNTR are shown respectively. Also shown in those figures are the conductance of (6,0) and (6,6) SWCNTs. The conductance of the respective CCNTR shows oscillations as a function of E because of the finite number of unit cells contained in the CCNTR. The conductance of the (6,0)-(6,6)/3648 CCNTR vanishes at the Fermi energy because the corresponding (6,6)/3648 CNTR is a small-gap semiconductor while that of the L(6,0)-T(6,6)/3672 CCNTR is at its peak value at the Fermi energy because the (6,6)/3672 CNTR is metallic. The overall peak conductance of the L(6,0)-T(6,6)/3672 CCNTR is seen to be exceeded by the overall peak conductance of the L(6,0)-T(6,6)/3648 CCNTR, even though the former corresponds to a metallic CNTR while the latter a small-gap semiconducting CNTR. This observation can be understood in terms of the contacts for the two cases. In the former case, the RJ is different from the LJ while in the latter

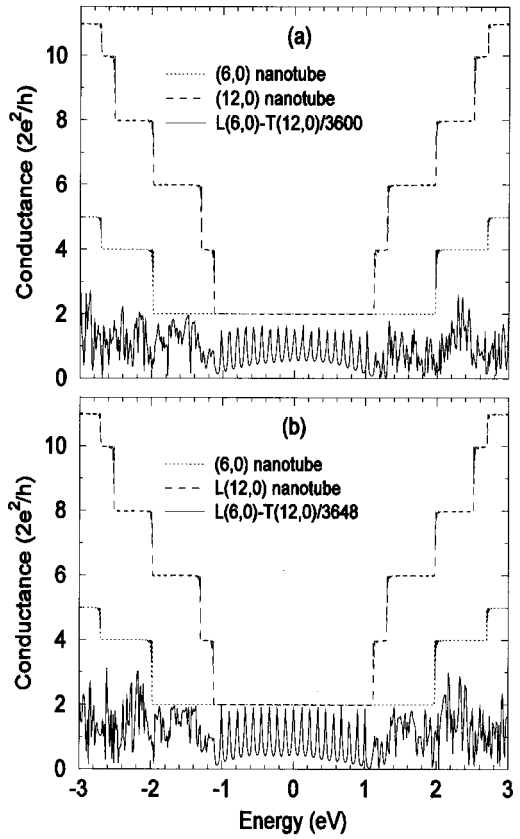

FIG. 5. Conductance of the L(6,0)-T(12,0) contacted CNTRI with (a) 3600 atoms and (b) 3648 atoms in the torus, respectively. Also shown are the conductance of the SWCNTs (6,0) and (12,0).

case, the two junctions are equivalent. The difference in the RJ and LJ will diminish the constructive quantum interference of the transmission as compared to the situation when the two junctions are equivalent. Another interesting observation is that the overall conductance seems to be following the conductance pattern of the (6,0) SWCNT rather than that of the (6,6) SWCNT. This feature can be understood in terms of the transport of the electrons from the lead into the sample and then out of the sample through the other lead. The transport is therefore controlled by the smaller number of channels of the leads and that of the sample. Since the (6,0) SWCNT leads have smaller number of channels compared to that of the sample, the conductance pattern of the CCNTR will follow the conductance pattern of the (6,0) SWCNT leads. Figures 5(a) and 5(b) display the conductance of the L(6,0)-T(12,0)/3600 and L(6,0)-T(12,0)/3648 CNTRI, together with that of the corresponding (6,0) and (12,0) SWCNTs. The conclusion drawn from the consideration of the (6,6) SWCNT-based CCNTRI in general applies also for the (12,0) SWCNT-based CCNTRI. It includes (1) the conductance achieves its peak value at the Fermi energy for both CCNTRI because both are metallic; (2) the overall peak conductance of the L(6,0)-T(12,0)/3600 CCNTR is smaller than that of the L(6,0)-T(12,0)/3648 CCNTR because the former has nonequivalent contacts while the latter has equivalent contacts; (3) the conductance pattern follows that of the leads. However, a closer examination of the figures shown in Figs. 4 and 5 reveal that the overall peak conductance of L(6,0)-T(12,0)/ CCNTRI is much higher compared to that of L(6,0)-T(6,6)/ CCNTRI. This can be understood because the contact between the (6,0) SWCNT lead and the (12,0) SWCNT-based CNTR is almost transparent (hence a peak conductance of $\sim 4e^2/h$) while that between the lead and the (6,6) SWCNT-based CNTR is not nearly so on account of the difference in their Fermi energy.

V. CONCLUSION

Our study clearly demonstrates that the conductance of a CCNTR depends on the transparency of the contact (chemistry) and whether the two leads are equivalent (chemistry as well as geometry). This conclusion is general and is expected to be applicable for any metallic contacts to the CCNTR.

The authors acknowledge the funding support from the NSF (Grants Nos: DMR-011282 and ECS-0224114), the U.S. DOE (Grant No. DE-FGO2-00ER45832), and also the support of National Science Council of Taiwan (Grants Nos: NSC 92-2120-M-002-003 and NSC 91-2112-M-054).

[1] J. Liu, H. Dai, J. H. Hafner, D. T. Colbert, R. E. Smalley, S. J. Tans, and C. Dekker, Nature (London) **385**, 780 (1997).
[2] M. Sano, A. Kamino, J. Okamura, and S. Shinkai, Science **293**, 1299 (2001).
[3] M. F. Lin and D. S. Chuu, Phys. Rev. B **57**, 6731 (1998).
[4] Lei Liu, G.-Y. Guo, C. S. Jayanthi, and S. Y. Wu, Phys. Rev. Lett. **88**, 217206 (2002).
[5] R. Saito, G. Dresseihaus, and M. S. Dresselhaus, *Physical Properties of Carbon Nanotubes*, fourth ed. (Imperial College, London, 1998).
[6] Lei Liu, C. S. Jayanthi, and S. Y. Wu, Phys. Rev. B **64**, 033412 (2001).
[7] C. S. Jayanthi, S. Y. Wu, J. Cocks, N. S. Luo, Z. L. Xie, M. Menon, and G. Yang, Phys. Rev. B **57**, 3799 (1998).
[8] S. Y. Wu and C. S. Jayanthi, Int. J. Mod. Phys. B **9**, 1869 (1995).
[9] Lei Liu, C. S. Jayanthi, M. Tang, S. Y. Wu, T. W. Tombler, C. Zhou, L. Alexseyev, J. Kong, and H. Dai, Phys. Rev. Lett. **84**, 4950 (2000).